Single Molecule Imaging of Green Fluorescent Proteins in Living Cells: E-Cadherin Forms Oligomers on the Free Cell Surface

Ryota Iino,* Ikuko Koyama,† and Akihiro Kusumi*†
*Kusumi Membrane Organizer Project, Exploratory Research for Advanced Technology Organization, Japan Science and Technology Corporation, Chiyoda 5-11-33, Nagoya 460-0012; and †Department of Biological Science, Nagoya University, Nagoya 464-8602, Japan

ABSTRACT Single green fluorescent protein (GFP) molecules were successfully imaged for the first time in living cells. GFP linked to the cytoplasmic carboxyl terminus of E-cadherin (E-cad-GFP) was expressed in mouse fibroblast L cells, and observed using an objective-type total internal reflection fluorescence microscope. Based on the fluorescence intensity of individual fluorescent spots, the majority of E-cad-GFP molecules on the free cell surface were found to be oligomers of various sizes, many of them greater than dimers, suggesting that oligomerization of E-cadherin takes place before its assembly at cell-cell adhesion sites. The translational diffusion coefficient of E-cad-GFP is reduced by a factor of 10 to 40 upon oligomerization. Because such large decreases in translational mobility cannot be explained solely by increases in radius upon oligomerization, an oligomerization-induced trapping model is proposed in which, when oligomers are formed, they are trapped in place due to greatly enhanced tethering and corralling effects of the membrane skeleton on oligomers (compared with monomers). The presence of many oligomers greater than dimers on the free surface suggests that these greater oligomers are the basic building blocks for the two-dimensional cell adhesion structures (adherens junctions).

INTRODUCTION

Technologies for observing single fluorescent molecules in solution have recently been developed, and are becoming very important tools in biophysics, biochemistry, and cell biology (Nie et al., 1994; Funatsu et al., 1995; Sase et al., 1995; Schmidt et al., 1996; Lu et al., 1998; Okada and Hirokawa, 1999; Weiss, 1999; Sako et al., 2000; Schütz et al., 2000). Another new important development in biological imaging is the specific labeling of proteins of interest in live cells using green fluorescent protein (GFP). Because the conjugation of GFP with a target protein is carried out at the cDNA level, and the GFP conjugate is expressed in cultured cells by transfecting cells with the cDNA plasmid, GFP labeling is particularly useful for the study of localization and mobility of the protein in living cells.

In 1997, three groups independently succeeded in imaging single GFP molecules in vitro (Pierce et al., 1997; Dickson et al., 1997; Iwane et al., 1997). However, single molecule GFP imaging has thus far been limited to isolated molecules from cells and studied in vitro (Pierce et al., 1997; Dickson et al., 1997; Iwane et al., 1997; Romberg et al., 1998; Pierce and Vale, 1999; Kubitscheck et al., 2000). Because the primary advantage of GFP conjugates is that they can be genetically expressed and imaged in living cells, extending the GFP technology to single molecule imaging in live cells is important. We report here the first observation of individual GFP molecules in living cells. We observed mutant GFP molecules linked to E-cadherin (E-cad-GFP), a calcium-dependent, cell-cell adhesion molecule. Using objective-type total internal reflection fluorescence microscopy, we were able to image individual E-cad-GFP molecules on the ventral cell membrane in live cells. The ventral surface (the membrane facing the coverslip rather than the culture medium) of L cells expressing E-cad-GFP models the basal membrane of simple epithelial cells, in which the major pool of E-cadherin before its assembly at the cell-cell contact sites is located.

E-cadherin is responsible for strong-type, cell-cell adhesion in epithelial and several other tissues. Cadherin family molecules carry out this function by assembling at the cell-cell contact sites (Takeichi, 1991; Gumbiner, 1996; Yeaman et al., 1999; Colman, 1999; Kusumi et al., 1999). To create adhesion sufficiently strong to prevent two adhered cells from being separated by forces acting from their environment, it has been proposed that E-cadherin molecules aggregate and anchor themselves to the actin filaments (Kusumi et al., 1990; Adams and Nelson, 1998; Shapiro and Colman, 1999; Kusumi et al., 1999; Gumbiner, 2000). The basic functional unit of cadherin has been proposed to be a dimer (Shapiro et al., 1995; Brieher et al., 1996; Takeda et al., 1999), based on the interaction in the first or the first and second homologous repeating extracellular domains of cadherin (Shapiro et al., 1995; Overduin et al., 1995; Nagar et al., 1996; Tamura et al., 1998; Pertz et al., 1999), as well as in the cytoplasmic (Ozawa and Kemler, 1998) and transmembrane (Huber et al., 1999) regions. In this model, an E-cadherin dimer in a cell membrane interacts with two dimers of an opposing cell, and by repeating such interactions, a zipper-like one-dimensional assembly of cadherin bridging the two cells is formed. However, none of these studies addressed the formation of greater oligomers, which may be necessary for the formation of the two-dimensional structures of cell-cell junctions (e.g., adherens junctions).

Received for publication 11 December 2000 and in final form 20 March 2001.

Address reprint requests to Akihiro Kusumi, Ph.D., Department of Biological Science, Nagoya University, Nagoya 464-8602, Japan. Tel: 81-52-789-2969; Fax: 81-52-789-2968; E-mail: akusumi@bio.nagoya-u.ac.jp.

0006-3495/01/06/2667/11 $2.00

Adams et al. (1998), using fluorescence microscopy of the E-cad-GFP, observed the formation of small puncta of E-cadherin at the cell-cell contact sites during the initial stages of cell-cell junction formation. The puncta are relatively small, two-dimensional assemblies of E-cadherin molecules (a few microns in diameter), and are likely to consist of E-cadherin from two apposing cells. The puncta move toward the edges of the cell-cell contact zone as the contact zone widens by a mechanism that involves actin filaments. Newly recruited E-cadherin molecules fill in as the puncta move. This observation clearly shows that the formation of E-cadherin oligomers is important for generation of adhesion at the junctions, and is a primary mechanism for the formation of junctions themselves. Therefore, the question of when, where, and how the oligomerization of E-cadherin occurs, and how such small oligomers are further assembled at the cell-cell contact sites, are critical issues in understanding the formation of cell-cell adhesion structures (Sako et al., 1998; Kusumi et al., 1999; Troyanovsky, 1999).

As a first step toward elucidation of these questions, we address the problem of the oligomerization levels of E-cadherin molecules on the free cell surface. Both in the presence and absence of E-cadherin-based intercellular junctions (adherens junctions), many E-cadherin molecules are found on the free surface (i.e., outside the cell-cell adhesion sites), where they function as a pool for the formation of intercellular junctions and survey new contacts with other cells (Sako et al., 1998; Adams et al., 1998; Kusumi et al., 1999; Koyama et al., 1999). Because the half-life of E-cadherin, even in the cellular junctions, is only ~5 h (Shore and Nelson, 1991), cells need a readily available pool of E-cadherin to maintain adherens junctions. In addition, E-cadherin on the free cell surface is likely to act as sensors of new physical contacts with other cells, surveying the free cell surface.

In our previous studies using single particle tracking and optical tweezers, we have shown that E-cadherin movement on the free cell surface is regulated by its interaction with the membrane skeleton. Such interaction involves tether (Fig. 1, *left*) and fence (Fig. 1, *right*) regulation of the membrane skeleton on E-cadherin movement (Kusumi et al., 1993; Sako et al., 1998; Kusumi et al., 1999). Because oligomerization of E-cadherin molecules is expected to increase their interactions with the membrane skeleton, understanding the degree of that oligomerization is particularly important for understanding the recruitment process of E-cadherin molecules from the free cell surface to the cell-cell junction sites.

To address this issue, we observed individual E-cad-GFP molecules in live cells, and examined the oligomerization levels of E-cadherin on the free cell surface. Even on the free cell surface, E-cad-GFP molecules were found to be in various oligomeric states, suggesting that oligomerization of E-cadherin takes place before its assembly at the cell-cell adhesion sites.

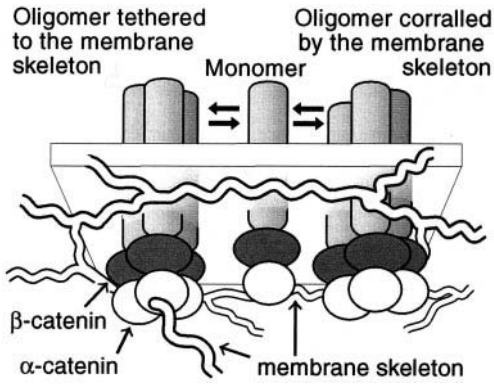

FIGURE 1 An oligomerization-induced trapping model. When oligomers are formed, they would be trapped in place due to the greatly increased effects of tethering and corralling by the membrane skeleton on oligomers compared to those on monomers (Kusumi and Sako; 1996; Sako et al., 1998; Kusumi et al., 1999). (*Left*) Oligomers are much more likely to be tethered to the membrane skeleton than monomers due to the multivalency (avidity) effects on binding and dissociation. (*Center*) Monomers would be relatively free from tethering to the membrane skeleton, and could readily hop from one compartment of the membrane skeleton mesh to an adjacent compartment. (*Right*) Oligomers are thought to hop to an adjacent compartment much more slowly than monomers because they have greater cytoplasmic domains.

Furthermore, oligomerization of E-cad-GFP molecules on the free cell surface was found to dramatically decrease their translational diffusion, strongly indicating a high degree of interaction with the membrane skeleton. Based on these observations, an oligomerization-induced trapping model is proposed, in which, in order to transmit the intracellular signal at the place where the extracellular signal is received, one of the major functions of the membrane skeleton mesh is to trap the receptor molecules (and the associated downstream intracellular signaling molecules) upon signal reception, after which oligomerization takes place (Fig. 1).

MATERIALS AND METHODS

Plasmid construction

The DNA fragment encoding full length E-cadherin (pBATEM2; provided by Dr. Nagafuchi, Kumamoto University; Nose et al., 1988), with the linker sequence 5′-GCTAGCATCGAATTCCCTAGAGGCGGCGGCGGC-3′ added to the 3′ end, was cloned into the bright mutant GFP expression vector pQBI25 (Quantum, Montreal, Canada) and was fused to the 5′ end of the GFP cDNA, yielding the E-cad-GFP expression vector (Koyama et al., 1999).

Cell culture and DNA transfection

L cells (a mouse fibroblast cell line) and Madin-Darby canine kidney epithelial cell line (MDCKII) cells were maintained in Ham's F12 medium (Life Technologies, Rockville, MD) and Dulbecco's modified Eagle's

medium (Life Technologies), respectively, and both were supplemented with 10% FBS (Sigma, St. Louis, MO). These cells were transfected using LipofectAMINE Plus (Life Technologies) according to the manufacturer's recommendations. Cells stably expressing E-cad-GFP molecules were selected with 0.3 mg/ml of G418, and positive clones were picked up with micropipettes. For fluorescence microscope imaging, cells were plated on coverslips and used 24 to 48 h later.

Single molecule imaging of E-cad-GFP

E-cad-GFP expressed on the ventral membrane of the cell (which faces the coverslip rather than the culture medium) was observed at 25°C with an objective-type total internal reflection fluorescence microscope (Tokunaga et al., 1997) that was constructed on an inverted microscope (Axiovert 135, Carl Zeiss) (Fig. 2). A 488 nm wavelength argon ion laser beam (Model 2013–75SL, Uniphase, San Jose, CA), attenuated with neutral density filters and circularly polarized by a quarter wave plate was expanded by two lenses (L1 and L2 in Fig. 2 *A*, f = 8 and 80 mm, respectively), focussed at the back-focal plane of the objective lens with an L3 lens (Fig. 2 *A*; f = 350 mm), and then steered onto the edge of a high numerical aperture objective lens (PlanApo100× ; numerical aperture = 1.4, Olympus). A 495-nm dichroic mirror (Q495LP; Chroma Technology, Brattleboro, VT) was used. The laser beam was totally internally reflected at the coverslip-medium interface (incident angle, 66°), and an evanescent field (1/*e* penetration depth, ~100 nm) was formed on the surface of the coverslip (Axelrod et al., 1984) (Fig. 2 *B*). For the measurement of the incident angle, the coverslip used to set up the condition of total internal reflection was replaced by a 45° dispersion prism, and the incident angle was calculated from the angle of the laser beam emitted from the prism. The ventral membranes were locally illuminated with this evanescent field. The illuminated area on the coverslip was ~130 μm^2. The incident laser power was set such that its power was 55 μW after passing through the objective lens (the incident angle, 0° for the measurement of the laser power). The stray excitation light was blocked with an interference bandpass filter of 500 to 550 nm (HQ525/50; Chroma) placed after the dichroic mirror. The fluorescence images were projected onto a microchannel plate intensifier (VS4–1845; Video Scope, Sterling, VA), and the intensified images were recorded at video rate by a silicon-intensified target tube (SIT) camera (C2400–08; Hamamatsu Photonics, Hamamatsu, Japan) and a digital video cassette recorder (DSR-20; Sony, Tokyo, Japan).

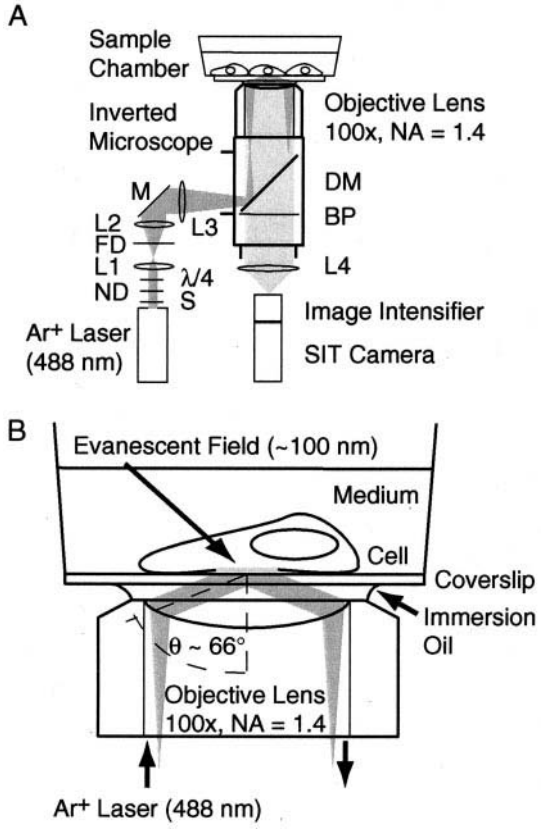

FIGURE 2 Schematic drawing of the objective-type total internal reflection fluorescence microscope used in this study. (*A*) Optical ray diagram. L1 and L2, beam expander ([10×); L3, focussing lens; L4, projection lens (4×); S, electronic shutter; ND, neutral density filter; λ/4, quarter-wave plate; FD, field diaphragm; DM, dichroic mirror; BP, bandpass filter; M, mirror. (*B*) Schematic drawing around the sample chamber and the objective lens. The argon ion laser beam (488 nm) was totally internally reflected at the coverslip-medium interface (the incident angle was set at 66°), and an evanescent field was formed (1/*e* penetration depth was ~100 nm).

Fluorescence intensity measurement

Fluorescence images were digitized frame by frame with an image processor (DVS-3000; Hamamatsu Photonics), and signal intensities of 408 nm × 408 nm areas (8-bit images in 7 × 7 pixels) containing a single spot were measured. To alleviate the adverse effect of shading (non-uniform sensitivity of the silicon-intensified target) of the SIT camera, only the central quarter of the image was used. As a control for single molecule imaging of GFP, GFP molecules extracted from *E. coli* transfected with GFP expression vector were non-specifically attached to the L cell surface from outside the cell, and to the coverslips (final concentration of GFP, 10 nM), and then imaged. Because GFP molecules attached to the coverslip were immobile, only mobile spots were considered to be truly attached to the L cell surface in order to convincingly identify them as such.

Analysis of E-cad-GFP movement

The trajectories of the fluorescent spots were obtained and analyzed by a published method (Kusumi et al., 1993; Sako et al., 1998). The positions (x and y coordinates) of each fluorescent spot were determined by an Intel Pentium III-based computer operating under Windows 98, using the method developed by Gelles et al. (1988). The accuracy of the position determination was estimated using immobile GFP molecules attached to the coverslip. The standard deviations of the measured coordinates were 19 nm horizontally and 21 nm vertically. The mean square displacement (MSD) was calculated for each time interval (Δt) over a trajectory, and the translational diffusion coefficient was calculated as the slope of the MSD-Δt plot between 100 and 333 ms (3 to 10 video frames) by least-square fitting (Kusumi et al., 1993). The median value of the nominal diffusion coefficient for the immobilized single GFP on the coverslip was 3.0×10^{-4} $\mu m^2/s$ (3.0×10^{-12} cm^2/s), which is the limit for determining the smallest diffusion coefficient under present instrumental conditions.

The movement of each spot was classified into stationary, simple, confined, or directed modes of diffusion (Kusumi et al., 1993). Because the nominal diffusion coefficient for the immobilized single GFP on the coverslip ranged between $\sim 5 \times 10^{-5}$ and $\sim 1 \times 10^{-3}$ $\mu m^2/s$ (5×10^{-13} and 1×10^{-11} cm^2/s), fluorescent spots that showed diffusion coefficients smaller than 1×10^{-3} $\mu m^2/s$ were classified into the stationary mode. Spots that exhibited the diffusion rates greater than 1×10^{-3} $\mu m^2/s$ were classified into simple, confined, or directed diffusion using a statistical method developed previously (Kusumi et al., 1993). Briefly, we employed $RD(100, 30)$ as a parameter to describe relative deviations, where $RD(N, n)$ is defined as

$$RD(N, n) = MSD(N, n)/4Dn\delta t,$$

where $MSD(N, n)$ represents MSD determined at the time interval $n\delta t$ (δt = 33 ms at video rate) from a sequence of N video frames, and $4Dn\delta t$ is the expected average value of MSD for $n\delta t$ s for a spot undergoing simple Brownian diffusion with a diffusion coefficient of D in two-dimensional space. In the case of simple diffusion, $RD(N, n)$ averaged over a sufficiently long trajectory for many particles should be 1. By simulating the movements of particles undergoing simple Brownian diffusion using a computer, we obtained the distribution of $RD(100, 30)$. $RD(100, 30)$ for each experimental trajectory was tested to determine whether this value fell within 2.5% from either end of the distribution of simulated particles. When $RD(100, 30)$ was within the middle 95% of the distribution, the trajectory was classified into simple Brownian diffusion. When $RD(100, 30)$ was within 2.5% from the low (high) end of the distribution of simulation, the trajectory was classified into confined (directed) diffusion.

Immunoblot analysis

Cells were solubilized with a cell lysis buffer [1% SDS, 25 mM Tris-HCl, 150 mM NaCl (pH 7.0)] supplemented with a protease inhibitor cocktail (Roche Diagnostics, Indianapolis, IN). Samples containing 20 μg of total protein were separated by sodium dodecyl sulfate-polyacrylamide gel electrophoresis and transferred to a nitrocellulose membrane. Bands of E-cadherin and E-cad-GFP were immunostained using a rat monoclonal anti-E-cadherin antibody ECCD-2 (a gift of hybridoma from Dr. M. Takeichi, Kyoto University) and an ECL PLUS detection system (Amersham, Buckinghamshire, United Kingdom).

RESULTS AND DISCUSSION

Characterization of E-cad-GFP expressing cells and the instrument

L cells were transfected with an expression vector encoding E-cad-GFP, and are called LEG cells in this report. LEG cells expressing low levels of E-cad-GFP (observed under an epi-fluorescence microscope) were selected and cloned to facilitate single molecule imaging (see the next section and Fig. 4) and to avoid associations of GFP portions of the E-cad-GFP and non-specific interactions among E-cad-GFPs (De Angelis et al., 1998). The expression of E-cad-GFP was detected by Western blotting using anti-E-cadherin antibody (Fig. 3). Wild-type L cells do not express detectable levels of endogenous E-cadherin, and do not form well developed adhesion structures. LEG cells cloned as above were further selected using Western blotting, and clones of a LEG cell expressing E-cad-GFP below 1% of the average level of endogenous E-cadherin expressed in MDCKII cells were used throughout the present research. The result of Western blotting of such LEG cells is shown in Fig. 3 (*lane 3*). However, even at such low levels of E-cad-GFP expression, LEG cells exhibited calcium-dependent cell-cell adhesion in a cell aggregation assay (Adams et al., 1998; Koyama et al., 1999; data not shown), and cobblestone-like morphology characteristic with epithelial cells and L cells expressing higher levels of E-cadherin (Sako et al., 1998), as well as concentration of E-cad-GFP at the cell-cell interfaces.

These cloned LEG cells were cultured on coverslips, and their ventral membranes (cell surface membranes facing the coverslip) were imaged using an objective-type total internal reflection fluorescence microscope (Fig. 4). This method has been used for imaging single fluorescent molecules in vitro (Funatsu et al., 1995; Tokunaga et al., 1997; Iwane et al., 1997; Pierce et al., 1997; Romberg et al., 1998; Pierce and Vale, 1999). In the present experiments, to enhance the fluorescence signal level, we employed a microchannel plate intensifier with a gallium-arsenide photo-

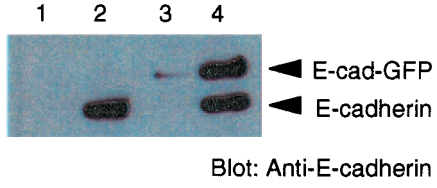

FIGURE 3 Expression of E-cadherin and E-cad-GFP detected by Western blotting using anti E-cadherin antibody (ECCD2). (*Lanes 1 and 2*) Wild-type L cells and wild-type MDCKII cells, respectively. (*Lane 3*) L cells expressing low levels of E-cad-GFP (LEG cell). (*Lane 4*) MDCKII cells transfected with E-cad-GFP, showing both endogenous E-cadherin and transfected E-cad-GFP.

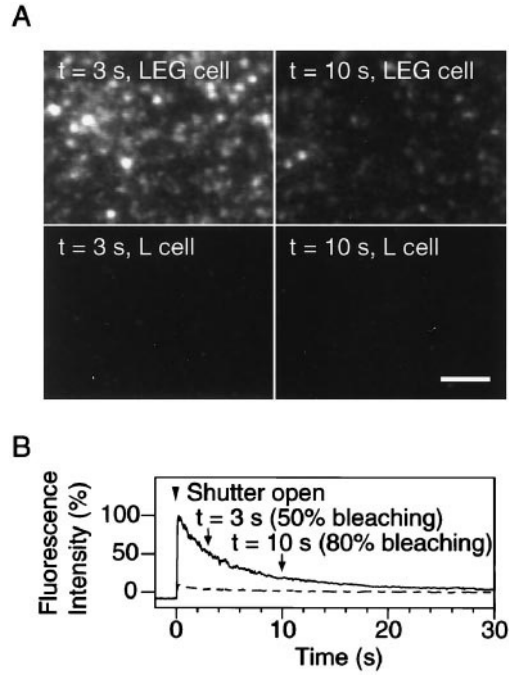

FIGURE 4 Single fluorescent-molecule imaging of E-cad-GFP on the ventral membrane of live transfected L cells using total internal reflection fluorescence microscopy. (*A*) Images of the ventral membrane of a LEG cell (*top row*) and a wild-type L cell (*bottom row*), acquired after 50% (*left column*, t = 3 s in B) and 80% (*right column*, t = 10 s in B) photobleaching of E-cad-GFP. Images were averaged over 8 video frames. Scale bar, 2 μm. (*B*) Typical decays of fluorescence intensity of 5.8 μm × 5.8 μm (100 × 100 pixels) areas by photobleaching, measured on a LEG cell and an L cell. Solid line, LEG cell; dashed line, wild-type L cell.

cathode, and an SIT camera. It was necessary to use higher intensifier gains to amplify the GFP signal than those used for Cy3 (a synthesized dye), which, in turn, necessitated keeping the sample environment (culture media and the coverslips) clean and maintaining good proliferative conditions for the cell (an increase in autofluorescence from the cytoplasmic fluid and an increase in the number of vesicles are typical with cells cultured under unfavorable conditions).

Imaging of single E-cad-GFP molecules on the cell membrane

Fig. 4 *A* shows fluorescence images of the ventral surface of the LEG and L cells. Individual fluorescent spots could not be discerned in the images of LEG cells acquired immediately after initiation of illumination, due to the overly abundant spots of E-cad-GFP present in the cell membrane (despite the selection of low expressers). Therefore, we observed the cells 3 and 10 s after the excitation light was turned on, at which 50 and 80% of the E-cad-GFP, respectively, were photobleached (Fig. 4 *B*, and it indicates GFP does not follow single-exponential photobleaching kinetics). The excitation power ($\sim$0.4 μW/μm^2) used here is comparable to that for normal epi-fluorescence observation of GFP, as judged by its photobleaching kinetics (1/e $\sim$10 s).

Under these conditions, E-cad-GFP molecules were observed as many spots with various fluorescence intensities. This suggests that E-cad-GFP molecules form oligomers. The expression levels of E-cad-GFP, as estimated from the fluorescence intensity, varied among LEG cells by $\pm\sim$50% of the mean level. In contrast, autofluorescence of L cells (Fig. 4 *A*, *bottom*) was low compared with the fluorescence intensity in LEG cells. These results are quantitatively shown in Fig. 4 *B*, in which the average fluorescence intensity in a 5.8 μm $\times$ 5.8 μm image area (100 $\times$ 100 pixels) is shown as a function of time after the initiation of illumination. The solid and dashed lines in Fig. 4 *B* show the decay of fluorescence intensities by photobleaching for LEG and L cells, respectively. Typical autofluorescence intensity of L cells was $<$10% of the fluorescence intensity of the LEG cells when compared immediately following the initiation of the observation (see Fig. 4 *B* near time 0).

In order to study the variations in the fluorescence intensity of each E-cad-GFP spot, we measured the fluorescence intensity of the individual spots at the average photobleaching levels of 50 and 80% (Fig. 5). First, we measured the intensities of autofluorescence of L cells by randomly selecting areas from their images. The measured intensity is thought to be the sum of the stray excitation light, fluorescence from the optical system, the thermal noise of the detector and the electronic system, and the real autofluorescence from the cell. Fig. 5 *A* shows the distribution of the autofluorescence intensity. Note that the mean value of the

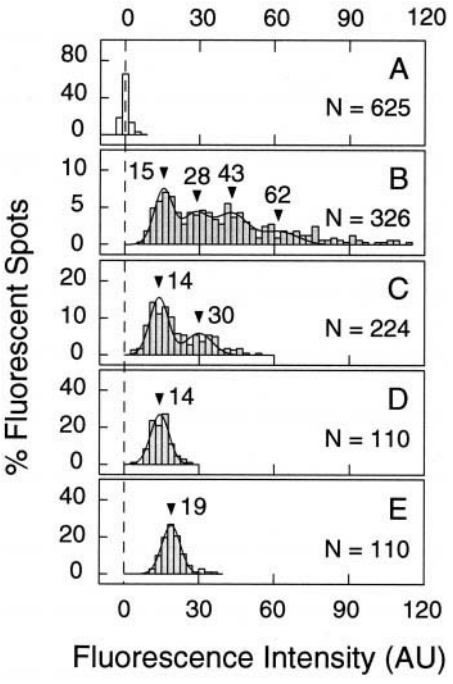

FIGURE 5 Distributions of fluorescence intensities of E-cad-GFP. Signal intensities of 408 nm $\times$ 408 nm areas (8-bit images in an area of 7 $\times$ 7 pixels) containing a single spot were measured. Note that the mean value of the background intensity for the wild-type L cells (7.6 $\pm$ 1.6 AU; N = 625) was always subtracted from the direct computer read-out values. (*A*) Distribution of the background intensity of the wild type L cells. (*B and C*) Distributions of fluorescence intensities of E-cad-GFP after 50% (*B*) and 80% (*C*) photobleaching. (*D and E*) Distributions of the fluorescence intensity of GFP molecules non-specifically attached to the ventral membrane of L cells (*D*) or coverslips (*E*). The solid lines in *B-E* show the fits by Gaussian functions. In *D* and *E*, the distribution was fitted with a single Gaussian function with dispersions (σ^2) of 13.8 and 14.3, respectively. In *B* (between 0 and 70 AU of the fluorescence intensity) and *C*, the quadruple and double Gaussian functions, respectively, were used for fitting by assuming the width evaluated in *D* (for the peaks representing apparent dimer and greater oligomers, the width was multiplied by the number of monomers in an oligomer). The positions and the peakheights were adjustable fit parameters. Correlation coefficients of the fitting were 0.94 (*B*), 0.90 (*C*), 0.97 (*D*), and 0.99 (*E*). Filled arrowheads indicate the peak positions (fluorescence intensities) of quantized peaks determined by the Gaussian fitting.

autofluorescence intensity (a direct computer read-out value of 7.6 $\pm$ 1.6 arbitrary unit [AU], N = 625; the same unit was used throughout this work) was set to zero in all the histograms shown in Fig. 5 (7.6 was always subtracted from the read-out values). The histograms for the fluorescence intensity of E-cad-GFP spots show distributions of quantized fluorescence intensities with a basic fluorescence intensity of around 15 AU for both 50 and 80% photobleaching (Figs. 5 *B* and *C*, respectively). At the level of 50% photobleaching (Fig. 5 *B*), the histogram exhibits a broad range of quantized intensities, including peaks which are 3- and 4-fold the basic fluorescence intensities. At the level of 80% photobleaching (Fig. 5 *C*), only those peaks with basic

and double intensities are apparent. These quantized distributions were fitted well by multiple Gaussian functions (solid lines in Figs. 5 *B* and *C*, see the legend for the method of fitting), which support the quantized distributions of fluorescence intensity of each fluorescent spot.

As a control for the imaging of individual GFP molecules, we observed GFP obtained from *E. coli* transfected with a GFP expression vector. Fig. 5 *D* and *E* show the histograms for the fluorescence intensities of GFP molecules non-specifically attached to the surface of L cells (from outside), and to the coverslips, respectively. The mean fluorescence intensity of GFP on the ventral cell surface was 15 AU ($N = 110$; Fig. 5 *D*). This value was comparable to that observed for the basal peak of E-cad-GFP molecules, indicating that the fluorescence intensity for the basal peak of the quantized distribution corresponds to the GFP monomer intensity. On the other hand, the mean fluorescence intensity of single GFP molecules on the coverslips (Fig. 5 *E*) was 19 (AU; $N = 110$), which is slightly higher than that of GFP on the cell surface. Because the intensity of the evanescent field decays exponentially as a function of the distance from the coverslip-medium interface (Axelrod et al., 1984), the higher intensity of GFP fluorescence on the glass surface compared with that on the cell surface is due to the distance between the GFP fluorophore and the glass-buffer interface being closer.

Our evidence for imaging of individual E-cad-GFP molecules are summarized below as follows. (1) The histograms for the fluorescence intensity of E-cad-GFP spots showed quantized peaks (Figs. 5 *B* and *C*). (2) The fluorescence intensity for the basal peak was comparable to that of single GFP molecules (produced in *E. coli*) non-specifically attached to the ventral membrane (Fig. 5 *D*). (3) Fluorescent spots with intensities of the basal peak (indicated by the single arrowhead in Fig. 6 *A*) showed single-step, quantized photobleaching during observation (Fig. 6 *B*). (4) The fluorescent spots showed large intensity fluctuations, which are consistent with the observations of single GFP molecules in vitro (Fig. 6 *B*) (Pierce et al., 1997; Dickson et al., 1997; Iwane et al., 1997; Pierce and Vale, 1999).

Taken together, it is concluded that GFP molecules were individually imaged in live cells, extending single fluorophore observations of GFP molecules from in vitro to in vivo. This is important because the primary advantage of GFP conjugates is that they can be genetically expressed in living cells. Single GFP imaging in live cells will allow one to study various molecules individually as they actually function, and will open new possibilities in the study of molecular mechanisms of cellular functions.

E-cad-GFP forms oligomers on the free cell surface

After 50% photobleaching, many remaining spots still showed a broad range of quantized fluorescence intensities, including that of the monomer (Fig. 5 *B*), indicating that many E-cad-GFP molecules form oligomers/aggregates greater than dimers, even when they are on the free surface, before their assembly at the cell-cell adhesion sites. However, the sizes of most oligomers are expected to be smaller than ~decamers, because the maximal intensity in the fluorescence intensity distribution at 50% bleaching (Fig. 5 *B*) corresponds to heptamers (~110 AU), and because the spots with intensities greater than that of dimers were rarely observed after 80% photobleaching (Fig. 5 *C*).

The expression level of E-cad-GFP in LEG cells was <1% of the average level of endogenous E-cadherin expressed in MDCKII cells (Fig. 3), suggesting that oligomerization of E-cad-GFP was not induced by GFPs. In other words, oligomerization of the wild-type E-cadherin is likely to occur under physiological conditions. Given much higher concentrations of E-cadherin in epithelial cells, there may be only low concentrations of monomers. In fact, when LEG cells that had higher expression levels of E-cad-GFP were observed, the distribution of the fluorescence intensity shifted toward higher values (data not shown). This result is consistent with the equilibrium formation of oligomers, which in turn suggests the presence of greater oligomers in normal epithelial cells.

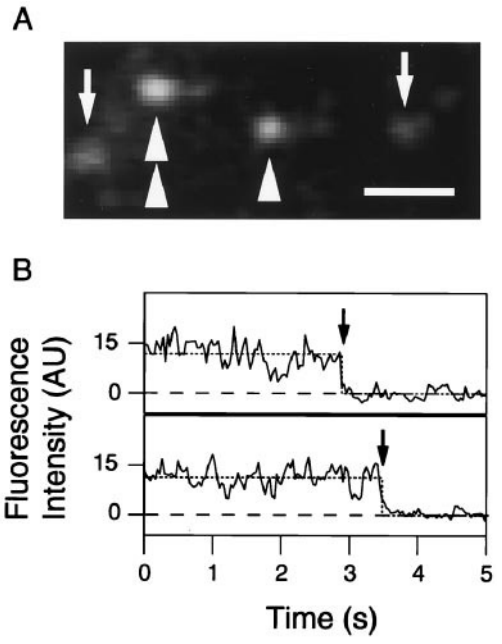

FIGURE 6 Single-step photobleaching of E-cad-GFP spots observed at video rate. (*A*) An image of immobile E-cad-GFP spots with basic (single arrowhead) and double quantized intensities (*double arrowheads*). Images were averaged over 8 video frames. Dimmer spots indicated by arrows represent diffusing spots blurred by frame averaging. Scale bar, 1 μm. (*B*) Typical examples of single-step photobleaching of the E-cad-GFP spots with basic quantized intensities. Photobleaching occurred at the time indicated by arrows. The average intensities of the spot and the background are shown by dotted and dashed lines, respectively.

One might think that the fluorescent spots with intensities greater than that of monomers are simply a result of the presence of two or more E-cad-GFP molecules that are coincidentally near enough to each other to be within the resolution of optical microscopy. However, we found that many such fluorescent spots were diffusing, and that most of those with intensities greater than that of dimers diffused as a unit (Fig. 7), rarely breaking up into smaller spots. These observations strongly support the assertion that the fluorescent spots with higher intensities are due to the presence of E-cad-GFP oligomers.

We do not think that these brighter spots represent E-cad-GFP molecules located in the intracellular vesicles (Le et al., 1999). These oligomers can be stained with Cy3-conjugated Fab fragments of an anti E-cadherin antibody added from outside the living cells (data not shown), clearly indicating that most of the E-cad-GFP is on the cell surface and is exposed to the culture medium.

Effect of E-cad-GFP oligomerization on its translational mobility

Fig. 7 shows an image of the E-cad-GFP fluorescence spots with various intensities along with their trajectories for 3.3 s (100 video frames), which were classified as exhibiting simple, confined, and stationary modes of diffusion. As the fluorescence intensity increases, the trajectories tend to exhibit less motion.

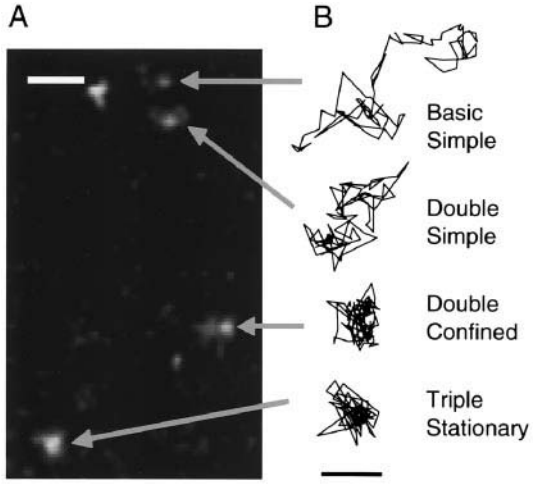

FIGURE 7 Correlations of the fluorescence intensities of the individual E-cad-GFP spots with their diffusion trajectories. (*A*) A fluorescence image of E-cad-GFP spots, showing basic, double, or triple quantized intensities. Scale bar, 1 μm. (*B*) Trajectories of E-cad-GFP spots shown in *A*, for 3.3 s (100 video frames). On their right, the quantized intensity (basic, double, triple) and the motional mode (simple, confined, stationary) of each spot are indicated. The trajectories of (Double, Confined) and (Triple, Stationary) may, at a first glance, appear similar, but the diffusion rates differ by a factor of 14 (7.2×10^{-3} and 5.2×10^{-4} $\mu m^2/s$, respectively). The central part of the (Triple, Stationary) trajectory is dense, because of a large decrease of the average diffusion rate, although the trajectory exhibits occasional large movements. However, due to such apparent similarity, we treat the trajectories classified into confined and stationary modes as a single group in this paper. Scale bar, 250 nm.

Fig. 8 shows the relationship between the diffusion coefficient and the fluorescence intensity of each spot. These spots are classified into four distinct species having monomer to tetramer fluorescence intensities as determined by the quantized distribution of the fluorescence intensity shown in Fig. 5 *B*. The boundaries between different quantized intensities are indicated by dashed vertical lines in Fig. 8. Note that these quantized intensities do not directly correlate with the oligomer size because images were taken after 50% of E-cad-GFP had been photobleached. Nevertheless, the fluorescence intensity of each E-cad-GFP spot tends to reflect the level of E-cad-GFP oligomerization, and thus provides a convenient yardstick for the degree of oligomerization. With an increase in the fluorescence intensity of the E-cad-GFP spots, particularly for those with trimer and tetramer intensities, the diffusion rates tend to decrease.

We also examined the mode of motion for individual spots. They were classified either into simple Brownian diffusion (52%, *filled circles* in Fig. 8) or confined + stationary modes of diffusion (48%, *open circles* in Fig. 8), based on the method described previously (Kusumi et al., 1993). E-cad-GFP spots defined to be in the stationary mode were those exhibiting diffusion coefficients less than 1×10^{-3} $\mu m^2/s$, which is the nominal diffusion coefficient (determined by the noise; the median value for the stationary mode was 3.0×10^{-4} $\mu m^2/s$)

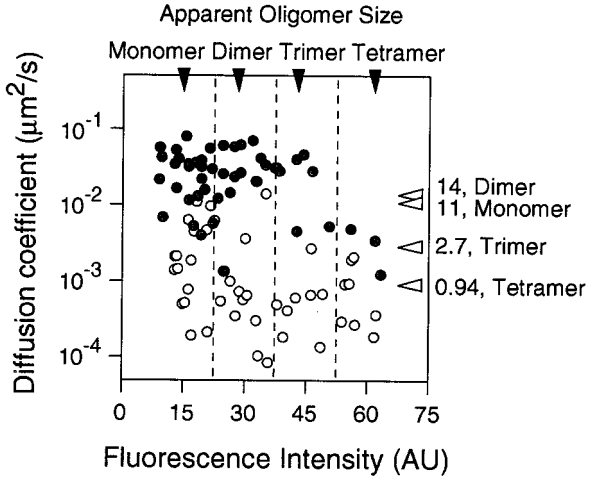

FIGURE 8 The diffusion coefficient plotted against the fluorescence intensity of each spot. Each spot was classified into the simple diffusion mode (*filled circles*) or the confined + stationary modes of diffusion (*open circles*). The intensity of each spot was defined to be the average over the first 8 video frames of each trajectory. Each spot was classified into four apparent oligomerization levels (monomers to tetramers). The boundaries between each level are shown by dashed vertical lines. Filled arrowheads indicate the peak positions in the fluorescence intensity histogram shown in Fig. 5 *B*. Open arrowheads indicate the median values of the diffusion coefficients for each intensity (oligomerization) level.

obtained for GFP molecules bound to the coverslip (for the details of the definition of the stationary mode, see Materials and Methods). None of the spots were classified into directed diffusion mode. As can be seen in Fig. 8, the spots exhibiting simple Brownian diffusion (*closed circles*) tend to have smaller oligomeric levels and greater diffusion coefficients, and those exhibiting confined + stationary modes (*open circles*) represent a greater fraction as the oligomerization level increases and tend to have smaller diffusion coefficients. This can be seen more clearly in Fig. 9*A*, in which the fractions of simple and confined + stationary modes are shown for each oligomeric state.

The distributions of the diffusion coefficient for each (apparent) oligomeric state are shown in Fig. 9 *B*, with a classification into simple (*filled bars*) and confined + stationary modes (*open bars*). With an increase in the level of oligomerization, the spots showing the confined + stationary modes increased, and at the same time those exhibiting the simple diffusion mode decreased, consistent with the result shown in Fig. 9 *A*. However, the median diffusion coefficient for each diffusion mode remained similar even when the apparent oligomerization level was different (in extreme cases, such as the monomers exhibiting the confined + stationary mode and the tetramers exhibiting the simple mode, diffusion rates which were either a little greater or somewhat smaller, respectively, were observed, probably due to incomplete separation of different diffusion modes). This result indicates that the decrease in the median diffusion coefficient for each apparent oligomerization level (without the distinction of motional modes, shown on the right side in Fig. 8) with a corresponding increase in the oligomer size reflects the shift of the populations between the two motional modes rather than a gradual decrease of the diffusion rate as the apparent oligomer size increases. The median diffusion coefficient for the E-cadherin-GFP molecules undergoing simple Brownian diffusion was 28×10^{-3} $\mu m^2/s$, while that for those undergoing diffusion of the confined + stationary mode was 0.71×10^{-3} $\mu m^2/s$ (see the value for Total at the bottom of Fig. 9 *B*), i.e., a difference of a factor of 40.

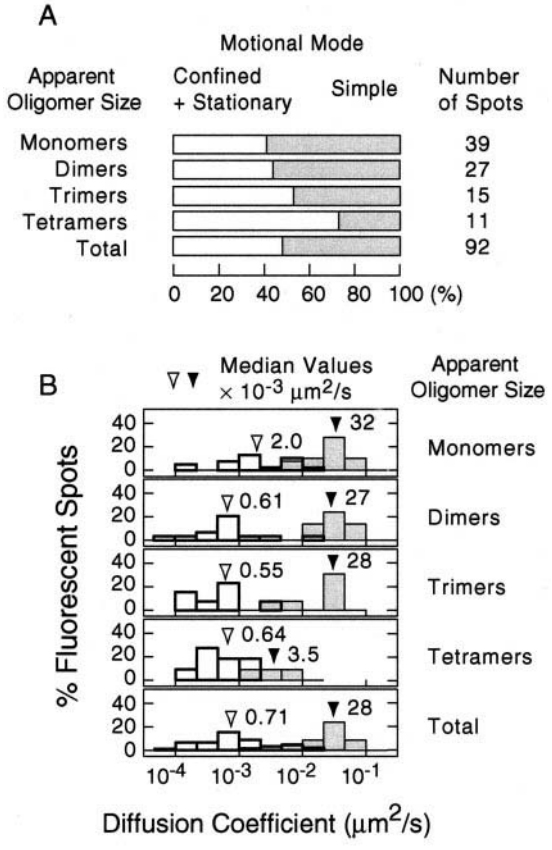

FIGURE 9 (*A*) Fractions of E-cad-GFP classified into simple and confined + stationary modes of diffusion for each (apparent) oligomer size (monomers to tetramers). (*B*) Distribution of the translational diffusion coefficient for E-cad-GFP as a function of apparent oligomerization levels and motional modes (simple or confined + stationary). Filled bars and open bars indicate simple diffusion and confined + stationary modes of diffusion, respectively.

Oligomerization-induced trapping of E-cadherin due to the interaction with the membrane skeleton

The above result is inconsistent with the general understanding of the translational diffusion rate of membrane-constituent molecules in a pure lipid bilayer, in which translational diffusion in two-dimensional space is rather insensitive to the change in the size of the diffusing unit (Saffmann and Delbrück, 1975). Formation of tetramers from monomers (an increase in radius by a factor of 2) would decrease the diffusion rate only by a factor of 1.1 (even for 100 mers, the diffusion rate would decrease only by a factor of 1.4), assuming the monomer radius of the membrane-spanning domain is 0.5 nm, a small decrease compared with a factor of 40 decrease observed here.

The complex characteristics of E-cad-GFP diffusion can be explained by assuming that there are interactions with the membrane skeleton network, which has confinement (fence) and binding (tether) effects on the movement of E-cad-GFP (Fig. 1; Kusumi and Sako, 1996; Sako et al., 1998; Kusumi et al., 1999). According to our previous findings, half of the wild-type E-cadherin molecules expressed in L cells are tethered to the membrane skeleton (or totally confined in the membrane skeleton meshes), and the other half are, although not directly bound to, corralled by the membrane skeleton fences (but undergoing inter-compartmental hop diffusion) (Sako et al., 1998). For the transmembrane proteins that are not directly bound to the membrane skeleton, the cell membrane is compartmentalized with regard to their lateral diffusion; they are temporarily confined in a compartment formed by the membrane skeleton mesh and occasionally hop to an adjacent compartment, and by repeating such confinement + hop movement,

the transmembrane proteins undergo macroscopic diffusion in the membrane (Sako and Kusumi, 1994, 1995; Kusumi and Sako, 1996; Kusumi et al., 1998; Sako et al., 1998; Tomishige et al., 1998; Tomishige and Kusumi, 1999). When such movements were observed at a low time resolution (33 ms, video rate) and a low spatial precision (19 nm in horizontal and 21 nm in vertical directions) for short durations (typically ~3.3 s) in single fluorophore observations, apparently simple and confined + stationary modes of diffusion were observed, probably because monomers and smaller oligomers were able to hop across the compartment boundaries more readily than larger oligomers (although individual compartments were hard to see due to the limitations of the instrument and sample). E-cad-GFP molecules located in an area where the membrane skeleton meshwork is less dense would collide with the membrane skeleton less often. Therefore these proteins are likely to exhibit a greater diffusion rate ($\sim 28 \times 10^{-3}$ $\mu m^2/s$) with the simple diffusion mode.

Greater oligomers would have much less chance of hopping to adjacent compartments, and as a result, they tend to exhibit a confined mode (or a stationary mode when they are trapped in a very small compartment). Furthermore, greater oligomers are more likely to be tethered to the membrane skeleton; their dissociation from the membrane skeleton would be much less likely to occur as compared with monomers because each cadherin monomer in the oligomer must dissociate from the membrane skeleton before the oligomer itself can detach. Therefore, greater oligomers are likely to show diffusion rates much lower than those of monomers and smaller oligomers (0.71×10^{-3} $\mu m^2/s$, 1/40 of that for monomers and smaller oligomers).

As is seen in Fig. 8, quite a few E-cad-GFP spots with lower fluorescence intensities exhibited smaller diffusion coefficients than those expected for monomers and dimers. These spots may represent greater oligomers in which all but one or two E-cad-GFP molecules were photobleached, or E-cad-GFP monomers or dimers that are either corralled by the dense parts of the membrane skeleton meshwork or tethered to it.

Based on these observations and arguments, we propose an oligomerization-induced trapping model (Fig. 1), in which there is a strong coupling of oligomerization of transmembrane proteins with the membrane skeleton's corralling and tethering effects. In this model, as soon as oligomers are formed, they would immediately be trapped due to the greatly increased effects of the tethering and corralling by the membrane skeleton on oligomers as compared with monomers. Monomers would be relatively free from tethering and would easily hop from one compartment (of the membrane skeleton mesh) to an adjacent one. Tethering would be greatly enhanced by the multivalency of oligomers to the membrane skeleton (avidity effect), and due to increased steric effect on oligomers, corralling would also be enhanced (Sako et al., 1998; Tomishige et al., 1998; Tomishige and Kusumi, 1999).

Such oligomerization-induced trapping would be particularly important for signaling that involves polarized changes of the cytoskeleton, such as cell-cell and cell-substrate adhesion, chemotaxis, and protrusion of processes. In these kinds of signaling, the receptor molecules memorize where they received the extracellular signal. Receptor oligomerization after signal reception is a common occurrence, and in the presence of the membrane skeletal fence, these oligomers are then trapped in place. In the absence of the membrane skeleton fence, such trapping would not occur because translational diffusion is minimally affected by oligomerization in the two-dimensional medium.

Such trapping may either stop or delay long-distance diffusion, depending on the time scales of observation as well as the level of energy barrier for inter-compartmental hop movement. Adams et al. (1998), using fluorescence recovery after photobleaching (FRAP) with a time scale of minutes, found that about 90% of E-cadherin in MDCK cells are mobile, whereas Sako et al. (1998), using single particle tracking whose time scale was about 10 s, found that about half of E-cadherin are mobile and the other half are either totally trapped in or bound to a membrane skeleton mesh in transfected L cells. The time scale for observation here is seconds and about half of E-cad-GFP has been classified into the stationary + confined diffusion mode, which is consistent with the observation by Sako et al. (1998). Taken together, these results indicate that the molecules totally confined by the membrane skeleton corrals during seconds to several tens of seconds may undergo a micron-scale (but slow) diffusion in 5 to 10 min.

Kucik et al. (1999) reported that the mobility of concanavalin A receptors on the keratocyte cell surface only weakly depends on the aggregate size (which was varied by using particles of various sizes), which cannot apparently be explained by the oligomerization-induced trapping model. Because the keratocyts are very mobile cells, the interaction between the membrane and the membrane skeleton may be totally different from that in normal cell lines in culture. In addition, because concanavalin A is tetravalent and binds to glycolipids, their results cannot simply be compared to ours.

Because E-cadherin-based cell-cell adhesion requires interactions with actin filaments, one of the most prominent constituents of the membrane skeleton, the enhanced interaction of E-cadherin oligomers with the actin-rich membrane skeleton must play an important role in the formation of cell-cell adhesion structures.

GENERAL DISCUSSION AND CONCLUSIONS

Imaging of single GFP molecules in live cells

Single GFP molecules were imaged for the first time in living cells. Because the main motivation for developing and extending GFP technologies is to visualize localization and movement of target proteins in living cells, extending

single fluorophore imaging technologies to GFPs in live cells is of particular importance.

Single GFP imaging in live cells has become possible by employing an objective-type total internal reflection fluorescence microscope equipped with a gallium-arsenide photocathode detector and a microchannel plate amplifier, followed by video rate imaging with an SIT camera. Cleanliness of the culture media and the coverslips, and keeping the cultured cells in healthy conditions were paramount for this endeavor. This study has established a benchmark for future application of single GFP imaging in live cells.

Mechanism of cadherin assembly at the cell-cell contact sites

Based on the single GFP imaging technique for live cells, oligomerization levels and the movement of E-cad-GFP were directly observed for the first time. More than 50% of the GFP spots exhibited fluorescence intensities greater than those for monomers, indicating that the majority of E-cad-GFP molecules are in oligomeric complexes of sizes ranging from dimers to decamers. No predominance of dimers was detected. Strand dimers (Shapiro et al., 1995; Nagar et al., 1996; Yap et al., 1997b; Tamura et al., 1998; Pertz et al., 1999) may form larger oligomers on the cell surface before forming the homophilic bond. Because the diffusion rate of E-cad-GFP measured in the present study exhibited a similar distribution to that found for the wild-type E-cadherin expressed in L cells (Sako et al., 1998), we propose that the wild-type E-cadherin molecules form oligomers on the free surface of living cells. This is consistent with observations that E-cadherin molecules associate with each other in the extracellular (Shapiro et al., 1995; Overduin et al., 1995; Nagar et al., 1996; Tamura et al., 1998; Pertz et al., 1999), the transmembrane (Huber et al., 1999), and the cytoplasmic (Ozawa and Kemler, 1998) domains. Due to the presence of at least three interaction sites, E-cadherin could form greater oligomers (trimers or greater) in the cell membrane by multiple interactions in various domains. Therefore, it is possible that the basic unit for the greater oligomers detected here is the E-cadherin dimers (Yap et al., 1997b).

E-cadherin is found on the free cell surface and in the cell-cell contact sites. The population of E-cadherin on the free cell surface is likely to provide the ready pool for new cell-cell adhesion, and to survey for new physical contacts with other cells. The forming of oligomers on the free surface before their assembly at the cell-cell contact sites may be important for detection of new cellular contacts and initiation of high affinity adhesion at new cellular contacts, and also for the rapid formation of cell-cell adhesion structures. The findings made here necessitate the modification of current working models for the assembly process of E-cadherin at the cell-cell contact sites. Previously, it was proposed that the basic unit size of E-cadherin on the cell surface is a dimer, and that based on the *trans*-interactions of the dimers between two opposing cells, a large assembly of E-cadherin connecting the two cells are formed. Our findings clearly indicate that E-cadherin is in oligomeric states which are often greater than dimers on the free cell surface (outside the cell-cell adhesion sites). Coupled with the intercellular cadherin-cadherin interactions, these greater cadherin oligomers would allow formation of large two-dimensional cadherin aggregates. The puncta observed by Adams et al. (1998) may represent such complexes formed from cadherin oligomers. The formation of these complexes is consistent with the cylinder/oligomer model for the organization of cadherins at the initial stages of cell-cell junction formation (Yap et al., 1997a), except that we could not detect a preference for the formation of lateral dimers.

E-cadherin molecules undergoing (apparent) simple diffusion may diffuse freely in the plasma membrane until they hit the newly forming puncta or junctions and become incorporated there. However, the diffusion rate of E-cadherin undergoing confined + stationary modes of diffusion (mostly greater oligomers) is so low that the above model of free diffusion and entrapment at the contact sites would not work well for greater oligomers (Kusumi et al., 1999). How cadherin oligomers are assembled in the cell-cell contact sites to form cell-cell adhesion structures would be an interesting subsequent research subject.

We thank Professors A. Nagafuchi at Kumamoto University School of Medicine, S. Tsukita at Kyoto University Medical School, other members of their laboratories for providing cDNA of E-cadherin and the technical help for construction of the E-cad-GFP expression vector. We also thank Professor W. J. Nelson at Stanford University School of Medicine and the members of Kusumi laboratory for their helpful discussion.

REFERENCES

Adams, C. L., Y. T. Chen, S. J. Smith, and W. J. Nelson. 1998. Mechanisms of epithelial cell-cell adhesion and cell compaction revealed by high-resolution tracking of E-cadherin-green fluorescent protein. *J. Cell Biol.* 142:1105–1119.

Adams, C. L., and W. J. Nelson. 1998. Cytomechanics of cadherin-mediated cell-cell adhesion. *Curr. Opin. Cell Biol.* 10:572–577.

Axelrod, D., T. P. Burghardt, and N. L. Thompson. 1984. Total internal reflection fluorescence. *Annu. Rev. Biophys. Bioeng.* 13:247–268.

Brieher, W. M., A. S. Yap, and B. M. Gumbiner. 1996. Lateral dimerization is required for the homophilic binding activity of C-cadherin. *J. Cell Biol.* 135:487–496.

Colman, D. R. 1999. Neuronal polarity and the epithelial metaphor. *Neuron.* 23:649–651.

De Angelis, D. A., G. Miesenböck, B. V. Zemelman, and J. E. Rothman. 1998. PRIM: proximity imaging of green fluorescent protein-tagged polypeptides. *Proc. Natl. Acad. Sci. U.S.A.* 95:12312–12316.

Dickson, R. M., A. B. Cubitt, R. Y. Tsien, and W. E. Moerner. 1997. On/off blinking and switching behaviour of single molecules of green fluorescent protein. *Nature.* 388:355–358.

Funatsu, T., Y. Harada, M. Tokunaga, K. Saito, and T. Yanagida. 1995. Imaging of single fluorescent molecules and individual ATP turnovers by single myosin molecules in aqueous solution. *Nature.* 374:555–559.

Gelles, J., B. J. Schnapp, and M. P. Sheetz. 1988. Tracking kinesin-driven movements with nanometre-scale precision. *Nature.* 331:450–453.

Gumbiner, B. M. 1996. Cell adhesion: the molecular basis of tissue architecture and morphogenesis. *Cell.* 84:345–357.

Gumbiner, B. M. 2000. Regulation of cadherin adhesive activity. *J. Cell Biol.* 148:399–403.

Huber, O., R. Kemler, and D. Langosch. 1999. Mutations affecting transmembrane segment interactions impair adhesiveness of E-cadherin. *J. Cell Sci.* 112:4415–4423.

Iwane, A. H., T. Funatsu, Y. Harada, M. Tokunaga, O. Ohara, S. Morimoto, and T. Yanagida. 1997. Single molecular assay of individual ATP turnover by a myosin-GFP fusion protein expressed in vitro. *FEBS Lett.* 407:235–238.

Koyama, I., A. Nagafuchi, S. Tsukita, and A. Kusumi. 1999. Location changes of E-cadherin and alpha-catenin during development and degradation of cell-cell adhesion. *Cell Struct. Funct.* 24:546.

Kubitscheck, U., O. Kückmann, and R. Peters. 2000. Imaging and tracking of single GFP molecules in solution. *Biophys. J.* 78:2170–2179.

Kucik, D. F., E. L. Elson, and M. P. Sheetz. 1999. Weak dependence of mobility of membrane protein aggregates on aggregate size supports a viscous model of retardation of diffusion. *Biophys. J.* 78:2170–2179.

Kusumi, A., and Y. Sako. 1996. Cell surface organization by the membrane skeleton. *Curr. Opin. Cell Biol.* 8:566–574.

Kusumi, A., Y. Sako, T. Fujiwara, and M. Tomishige. 1998. Application of laser tweezers to studies of the fences and tethers of the membrane skeleton that regulate the movements of plasma membrane proteins. *In* Laser Tweezers in Cell Biology. M. P. Sheetz, editor. Academic Press, San Diego, CA. pp. 173–194.

Kusumi, A., Y. Sako, and M. Yamamoto. 1993. Confined lateral diffusion of membrane receptors as studied by single particle tracking (nanovid microscopy). Effects of calcium-induced differentiation in cultured epithelial cells. *Biophys. J.* 65:2021–2040.

Kusumi, A., K. Suzuki, and K. Koyasako. 1999. Mobility and cytoskeletal interactions of cell adhesion receptors. *Curr. Opin. Cell Biol.* 11:582–590.

Kusumi, A., A. Tsuji, M. Murata, Y. Sako, S. Kagiwada, T. Hayakawa, and S. Ohnishi. 1990. Development of time-resolved microfluorimetry and its application to studies of cellular membranes. *In* Time-Resolved Laser Spectroscopy in Biochemistry II. Vol. 1204. J. R. Lakowicz, editor. SPIE Press, Bellingham, WA. 776–783.

Le, T. L., A. S. Yap, and J. L. Stow. 1999. Recycling of E-cadherin: a potential mechanism for regulating cadherin dynamics. *J. Cell Biol.* 146:219–232.

Lu, H. P., L. Xun, and X. S. Nie. 1998. Single-molecule enzymatic dynamics. *Science.* 282:1877–1882.

Nagar, B., M. Overduin, M. Ikura, and J. M. Rini. 1996. Structural basis of calcium-induced E-cadherin rigidification and dimerization. *Nature.* 380:360–364.

Nie, S., D. T. Chiu, and R. N. Zare. 1994. Probing individual molecules with confocal fluorescence microscopy. *Science.* 266:1018–1021.

Nose, A., A. Nagafuchi, and M. Takeichi. 1988. Expressed recombinant cadherins mediate cell sorting in model systems. *Cell.* 54:993–1001.

Okada, Y., and N. Hirokawa. 1999. A processive single-headed motor: kinesin superfamily protein KIF1A. *Science.* 283:1152–1157.

Overduin, M., T. S. Harvey, S. Bagby, K. I. Tong, P. Yau, M. Takeichi, and M. Ikura. 1995. Solution structure of the epithelial cadherin domain responsible for selective cell adhesion. *Science.* 267:386–389.

Ozawa, M., and R. Kemler. 1998. The membrane-proximal region of the E-cadherin cytoplasmic domain prevents dimerization and negatively regulates adhesion activity. *J. Cell Biol.* 142:1605–1613.

Pertz, O., D. Bozic, A. W. Koch, C. Fauser, A. Brancaccio, and J. Engel. 1999. A new crystal structure, Ca^{2+} dependence and mutational analysis reveal molecular details of E-cadherin homoassociation. *EMBO J.* 18:1738–1747.

Pierce, D. W., N. Hom-Booher, and R. D. Vale. 1997. Imaging individual green fluorescent proteins. *Nature.* 388:338.

Pierce, D. W., and R. D. Vale. 1999. Single-molecule fluorescence detection of green fluorescence protein and application to single-protein dynamics. *In* Green Fluorescent Proteins. K. F. Sullivan and S. A. Kay, editors. Academic Press, San Diego, CA. 49–73.

Romberg, L., D. W. Pierce, and R. D. Vale. 1998. Role of the kinesin neck region in processive microtubule-based motility. *J. Cell Biol.* 140: 1407–1416.

Saffman, P. G., and M. Delbrück. 1975. Brownian motion in biological membranes. *Proc. Natl. Acad. Sci. U.S.A.* 72:3111–3113.

Sako, Y., and A. Kusumi. 1994. Compartmentalized structure of the plasma membrane for receptor movements as revealed by a nanometer-level motion analysis. *J. Cell Biol.* 125:1251–1264.

Sako, Y., and A. Kusumi. 1995. Barriers for lateral diffusion of transferrin receptor in the plasma membrane as characterized by receptor dragging by laser tweezers: fence versus tether. *J. Cell Biol.* 129:1559–1574.

Sako, Y., S. Minoghchi, and T. Yanagida. 2000. Single-molecule imaging of EGFR signalling on the surface of living cells. *Nat. Cell Biol.* 2:168–172.

Sako, Y., A. Nagafuchi, S. Tsukita, M. Takeichi, and A. Kusumi. 1998. Cytoplasmic regulation of the movement of E-cadherin on the free cell surface as studied by optical tweezers and single particle tracking: corralling and tethering by the membrane skeleton. *J. Cell Biol.* 140: 1227–1240.

Sase, I., H. Miyata, J. E. Corrie, J. S. Craik, and K. Kinosita, Jr. 1995. Real time imaging of single fluorophores on moving actin with an epifluorescence microscope. *Biophys. J.* 69:323–328.

Schmidt, T., G. J. Schütz, W. Baumgartner, H. J. Gruber, and H. Schindler. 1996. Imaging of single molecule diffusion. *Proc. Natl. Acad. Sci. U.S.A.* 93:2926–2929.

Schütz, G. J., G. Kada, V. Ph. Pastushenko, and H. Schindler. 2000. Properties of lipid microdomains in a muscle cell membrane visualized by single molecule microscopy. *EMBO J.* 19:892–901.

Shapiro, L., and D. R. Colman. 1999. The diversity of cadherins and implications for a synaptic adhesive code in the CNS. *Neuron.* 23:427–430.

Shapiro, L., A. M. Fannon, P. D. Kwong, A. Thompson, M. S. Lehmann, G. Grubel, J. F. Legrand, J. Als-Nielsen, D. R. Colman, and W. A. Hendrickson. 1995. Structural basis of cell-cell adhesion by cadherins. *Nature.* 374:327–337.

Shirayoshi, Y., A. Nose, K. Iwasaki, and M. Takeichi. 1986. N-linked oligosaccharides are not involved in the function of a cell-cell binding glycoprotein E-cadherin. *Cell Struct. Funct.* 11:245–252.

Shore, E. M., and W. J. Nelson. 1991. Biosynthesis of the cell adhesion molecule uvomorulin (E-cadherin) in Madin-Darby canine kidney epithelial cells. *J. Biol. Chem.* 266:19672–19680.

Takeda, H., Y. Shimoyama, A. Nagafuchi, and S. Hirohashi. 1999. E-cadherin functions as a cis-dimer at the cell-cell adhesive interface in vivo. *Nat. Struct. Biol.* 6:310–312.

Takeichi, M. 1991. Cadherin cell adhesion receptors as a morphogenetic regulator. *Science.* 251:1451–1455.

Tamura, K., W. S. Shan, W. A. Hendrickson, D. R. Colman, and L. Shapiro. 1998. Structure-function analysis of cell adhesion by neural (N-) cadherin. *Neuron.* 20:1153–1163.

Tokunaga, M., K. Kitamura, K. Saito, A. H. Iwane, and T. Yanagida. 1997. Single molecule imaging of fluorophores and enzymatic reactions achieved by objective-type total internal reflection fluorescence microscopy. *Biochem. Biophys. Res. Commun.* 235:47–53.

Tomishige, M., and A. Kusumi. 1999. Compartmentalization of the erythrocyte membrane by the membrane skeleton: intercompartmental hop diffusion of band 3. *Mol. Biol. Cell.* 10:2475–2479.

Tomishige, M., Y. Sako, and A. Kusumi. 1998. Regulation mechanism of the lateral diffusion of band 3 in erythrocyte membranes by the membrane skeleton. *J. Cell Biol.* 142:989–1000.

Troyanovsky, S. M. 1999. Mechanism of cell-cell adhesion complex assembly. *Curr. Opin. Cell Biol.* 11:561–566.

Weiss, S. 1999. Fluorescence spectroscopy of single biomolecules. *Science.* 283:1676–1683.

Yap, A. S., W. M. Brieher, and B. M. Gumbiner. 1997a. Molecular and functional analysis of cadherin-based adherens junctions. *Annu. Rev. Cell Dev. Biol.* 13:119–146.

Yap, A. S., W. M. Brieher, M. Pruschy, and B. M. Gumbiner. 1997b. Lateral clustering of the adhesive ectodomain: a fundamental determinant of cadherin function. *Curr. Biol.* 7:308–315.

Yeaman, C., K. K. Grindstaff, and W. J. Nelson. 1999. New perspectives on the mechanisms involved in generating epithelial cell polarity. *Physiol. Rev.* 79:73–98.